

Article

Mixed Oxime-Functionalized IL/16-s-16 Gemini Surfactants System: Physicochemical Study and Structural Transitions in the Presence of Promethazine as a Potential Chiral Pollutant

Subhashree Jayesh Pandya ¹, Illia V. Kapitanov ^{2,†} , Manoj Kumar Banjare ^{1,3} , Kamalakanta Behera ⁴ , Victor Borovkov ^{2,*} , Kallol K. Ghosh ^{1,*} and Yevgen Karpichev ^{2,*}

¹ School of Studies in Chemistry, Pt. Ravishankar Shukla University, Raipur 492010, India; subhashree210490@gmail.com (S.J.P.); manojbanjare7@gmail.com (M.K.B.)

² Department of Chemistry and Biotechnology, Tallinn University of Technology (TalTech), 12618 Tallinn, Estonia; illia.kapitanov@taltech.ee

³ MATS School of Sciences, MATS University, Pagariya Complex, Pandri, Raipur 492001, India

⁴ Department of Applied Chemistry (ASAS), Amity University, Gurgaon 122413, India; kamala.iitd@gmail.com

* Correspondence: victor.borovkov@taltech.ee (V.B.); kallolkghosh@gmail.com (K.K.G.); yevgen.karpichev@taltech.ee (Y.K.); Tel.: +91-771-2263146 (K.K.G.); +372-620-4381 (Y.K.)

† Current Address: Gemini Pharm Chem Mannheim GmbH, 68305 Mannheim, Germany.

Abstract: The increasing concern about chiral pharmaceutical pollutants is connected to environmental contamination causing both chronic and acute harmful effects on living organisms. The design and application of sustainable surfactants in the remediation of polluted sites require knowledge of partitioning between surfactants and potential pollutants. The interfacial and thermodynamic properties of two gemini surfactants, namely, alkanediyi- α,ω -bis(dimethylhexadecyl ammonium bromide) (16-s-16, where $s = 10, 12$), were studied in the presence of the inherently biodegradable oxime-functionalized ionic liquid (IL) 4-((hydroxyimino)methyl)-1-(2-(octylamino)-2-oxoethyl)pyridin-1-ium bromide (4-PyC8) in an aqueous solution using surface tension, conductivity, fluorescence, FTIR and ¹H NMR spectroscopic techniques. The conductivity, surface tension and fluorescence measurements indicated that the presence of the IL 4-PyC8 resulted in decreasing CMC and facilitated the aggregation process. The various thermodynamic parameters, interfacial properties, aggregation number and Stern–Volmer constant were also evaluated. The IL 4-PyC8-gemini interactions were studied using DLS, FTIR and NMR spectroscopic techniques. The hydrodynamic diameter of the gemini aggregates in the presence of promethazine (PMZ) as a potential chiral pollutant and the IL 4-PyC8 underwent a transition when the drug was added, from large aggregates (270 nm) to small micelles, which supported the gemini:IL 4-PyC8:promethazine interaction. The structural transitions in the presence of promethazine may be used for designing systems that are responsive to changes in size and shape of the aggregates as an analytical signal for selective detection and binding pollutants.

Keywords: mixed surfactant system; ionic liquid; gemini surfactants; chiral pollutants; promethazine; dynamic light scattering



Citation: Pandya, S.J.; Kapitanov, I.V.; Banjare, M.K.; Behera, K.; Borovkov, V.; Ghosh, K.K.; Karpichev, Y. Mixed Oxime-Functionalized IL/16-s-16 Gemini Surfactants System: Physicochemical Study and Structural Transitions in the Presence of Promethazine as a Potential Chiral Pollutant. *Chemosensors* **2022**, *10*, 46. <https://doi.org/10.3390/chemosensors10020046>

Academic Editor: Núria Serrano

Received: 30 November 2021

Accepted: 17 January 2022

Published: 25 January 2022

Publisher's Note: MDPI stays neutral with regard to jurisdictional claims in published maps and institutional affiliations.



Copyright: © 2022 by the authors. Licensee MDPI, Basel, Switzerland. This article is an open access article distributed under the terms and conditions of the Creative Commons Attribution (CC BY) license (<https://creativecommons.org/licenses/by/4.0/>).

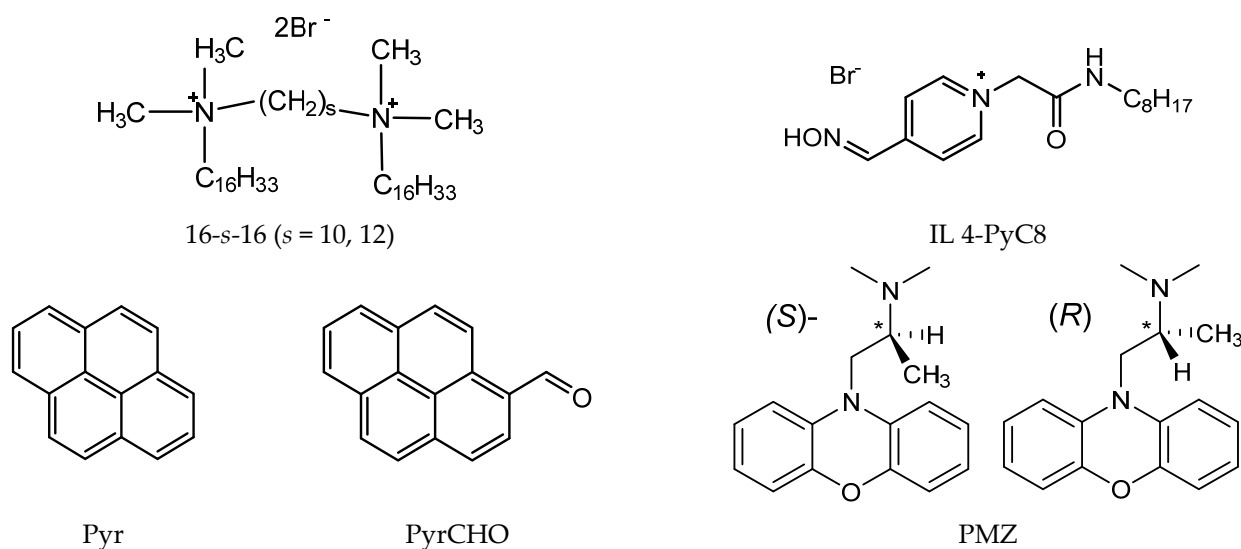
1. Introduction

The increasing concern about chiral pharmaceutical pollutants is connected to environmental contamination causing both chronic and acute harmful effects on living organisms. It is a problem of direct importance to detect chiral compounds [1], including chiral pollutants of different natures [2]. Using surfactants for increasing analytical signals and, consequently, reducing the detection concentration of the pollutants is one of the attractive strategies in chemical analysis [3,4] since it may ensure selective binding of one of the components, providing more reliable detection in the cases when the structurally similar compounds are present in the mixture. For example, dimeric (gemini) surfactants were reported to exhibit selectivity toward the binding of calixarenes modified with different

amino acid (L-Ala and L-Val) moieties [5]. An additional tool to evaluate the presence of a pollutant may be provided based on the sensitivity of self-assembly aggregates to the binding of target compounds, causing structural rearrangement of the aggregate's type, size and shape. Surfactant-based systems can effectively remove pollutant residues from surfaces of various types [6]. The design and application of sustainable surfactants in the remediation of polluted sites require knowledge of the interaction between surfactants and potential pollutants. Recently, environmentally friendly ionic liquids (ILs) have emerged as a novel system for the studies of green chemistry and environmental sciences [7–9]. ILs have been used significantly in organic synthesis [10,11], drug delivery [12], catalysis [13–15], separation processes [16,17] and the preparation of nanostructured materials [18]. The development of biocompatible and biodegradable ILs results in finding sustainable fragments to assist the synthesis of sustainable molecular blocks [19]. Garcia et al. [20] reported the micellization behavior and antimicrobial properties of ester- and amide-functionalized [21] pyridinium and imidazolium ILs with respect to the length of the side chain. Introducing an amide group in lieu of an ester group increases the stability of the functionalized ILs toward abiotic hydrolysis and thus extends the range of conditions of their practical application. A versatile approach included introducing an amino acid moiety to link the head group and side chain in the cation of IL/surface-active IL (SAIL) [19,22], which opened an opportunity to develop SAILs with optimized environmental toxicity [23], self-assembly [24] and biodegradability [25] properties. We recently reported the synthesis and study of a series of inherently biodegradable oxime-functionalized ILs [26] proposed as a base for a green decontamination IL–surfactant system. Although it is a well-established fact that the properties of ILs can be tuned with surfactants [27–29], using nonconventional surfactants (e.g., gemini surfactants) calls for more broad and detailed studies [30,31]. The gemini surfactants consist of two hydrophilic head groups and two hydrophobic chains covalently connected through a spacer group [32–34]. They have generated much interest because of their outstanding properties and their diverse applications compared with single-chain surfactants [25,26]. The aggregation behavior of monomeric conventional surfactants is mainly driven by intermolecular interactions, whereas a gemini surfactant is controlled by both inter-molecular and intra-molecular interactions. The physicochemical and interfacial properties of gemini surfactants in an aqueous solution depends upon the concentration, temperature, nature of hydrophobic tails, spacer properties and additives. Gemini surfactants have been studied to shed light on the effect of structural variation of surfactants on their binding ability with drugs, which, in turn, may also open new approaches for designing tunable drug carrier systems [35]. A mixed system of surfactant and ILs/SAILs with distinct morphology and physicochemical properties improves their performance in terms of cooperative combination [27–31]. The IL–surfactant interaction plays a crucial role for some applications in pharmaceutical and biomedical science, namely, in enhancing the permeability of drugs across biological membranes [36]. Ozan [37] described the effect of the imidazolium ILs EmimCl and BmimCl on the interaction and binding properties of phenothiazine and trifluopromazine hydrochloride with a series of nonionic surfactants (Brij 30, Brij 35 and Brij 56). Mahajan et al. [38] studied the micellization and interfacial behavior of a SAIL (C₁₄mimBr) and TTAB in the presence of drugs (dopamine hydrochloride and acetylcholine chloride) using conductivity and surface tension measurements. The binding constant and the Gibbs free energy change (ΔG) for the drug–surfactant complexes were evaluated via cyclic voltammeter measurements. Another work of this group [39] reported aggregation behavior of a series of novel SAILs, namely, diazabicyclo[5.4.0]undec-7-en-8-ium salts, and their interaction with the amphiphilic drug amitriptyline hydrochloride, indicating attractive interactions for the drug and SAILs. Recently, we reported the binding affinity of an inherently biodegradable oxime-functionalized SAIL with the phenothiazine drug promazine hydrochloride [40].

The present study aimed to shed light on surfactant systems containing gemini surfactants, a functionalized SAIL and an antidepressant drug promethazine hydrochloride (PMZ). The interfacial and thermodynamic properties of binary combinations of gemini

surfactants alkanediyl- α,ω -bis (dimethylhexadecyl ammonium bromide) (16-*s*-16, where *s* = 10, 12) (Scheme 1) with functionalized IL 4-((hydroxyimino) methyl)-1-(2-(octylamino)-2-oxoethyl) pyridin-1-iumbromide (4-PyC8), were studied using surface tension, conductivity, fluorescence, FTIR and ^1H NMR techniques. The effect of 4-PyC8 on the aggregation behavior, i.e., critical micelle concentration (CMC), surface excess concentration (Γ_{max}), surface pressure at CMC (π_{cmc}) and minimum area per molecule (A_{min}), were determined using the surface tension method. The thermodynamic parameters, i.e., the standard Gibbs free energy of aggregation ($\Delta G_{\text{m}}^{\circ}$), Gibbs energy of adsorption ($\Delta G_{\text{ads}}^{\circ}$), Gibbs energy of transfer ($\Delta G_{\text{trans}}^{\circ}$), Gibbs energy of micellization per alkyl tail ($\Delta G_{\text{tail}}^{\circ}$) and air–water interface ($\Delta G_{\text{min}}^{\text{s}}$), were evaluated using a conductometric technique. The CMC, aggregation number (N_{agg}) and Stern-Volmer constant (K_{sv}) were also determined via a fluorescence method using pyrene (Pyr) and 1-pyrene carboxaldehyde (PyrCHO) as the probes. FTIR and NMR techniques were successfully used to study the IL 4-PyC8:gemini interactions. The sizes of the gemini aggregates in the presence of PMZ and IL 4-PyC8 were studied using dynamic light scattering (DLS).



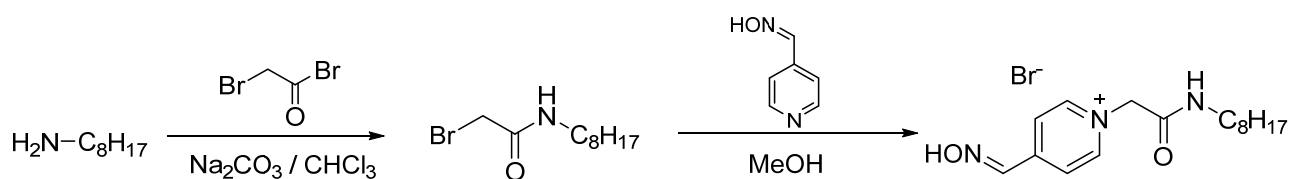
Scheme 1. Structures of the gemini surfactants (16-*s*-16), IL (4-PyC8) and fluorescent probes (Pyr and PyrCHO) studied in the present work, as well as the *S*- (left) and *R*- (right) enantiomers of promethazine (PMZ).

The structures of the gemini surfactants (16-*s*-16), conventional single-chain cationic surfactant cetylpyridinium chloride (CPC), functionalized IL 4-PyC8, antidepressant drug promethazine hydrochloride (PMZ) and fluorescent probes (Pyr and PyrCHO) used in the present study are shown in Scheme 1.

2. Experimental Section

2.1. Materials

1-Pyrene carboxaldehyde (PyrCHO), pyrene (Pyr), potassium chloride, cetylpyridinium chloride (CPC), promethazine hydrochloride (PMZ) and organic solvents were purchased from Sigma Aldrich. The PyCHO solutions were prepared in pure methanol. All the chemicals were used without further purification. The gemini surfactants alkanediyl-1,4-bis(dimethylhexadecyl ammonium bromide) 16-10-16 and 16-12-16 were synthesized by refluxing the corresponding decanediyl-1,10-*bis*-(cetyldimethylammonium bromide) in dry ethanol for 48 h, followed by recrystallization from hexane/ethyl acetate mixtures [29]. The IL 4-((hydroxyimino)methyl)-1-(2-(octylamino)-2-oxoethyl) (4-PyC8) was synthesized as described in our previous work [26] (see Scheme 2).



Scheme 2. Synthesis of IL 4-((hydroxyimino)methyl)-1-(2-(octylamino)-2-oxoethyl) (4-PyC8).

2.2. Methods

2.2.1. Conductivity

A digital conductivity meter (Systronics, Type 304) equipped with a conductivity cell of cell constant 1.01 cm^{-1} was used to measure the conductance for pure and mixed systems. The conductivity cell was calibrated before the measurements with standard solutions of potassium chloride (KCl) across a 0.01 M to 0.1 M concentration range. A concentrated gemini surfactant stock solution (10–20 times of the CMC) was progressively added using a micropipette to the IL 4-PyC8 solution. After thorough mixing and temperature equilibration at 300 K, the observed conductance was measured at each addition. The breakpoint of the plot of specific conductivity (κ) versus gemini surfactant concentration corresponded to the CMC for the pure gemini surfactant and mixed systems.

2.2.2. Surface Tension Measurements

The surface tension at different concentrations of gemini surfactants in the IL 4-PyC8 media was measured by using a KYOWA automatic surface tensiometer (DY-300) equipped with a platinum ring. The platinum ring was dried using a burner after every measurement to remove the sublimate of the gemini surfactant and the IL 4-PyC8. The surface tensiometer was calibrated by taking the surface tension of Millipore water ($72 \text{ mN}\cdot\text{m}^{-1}$ at 300 K). A 10 mL sample of 4-PyC8 solution was taken in a double-wall jacketed container, and the concentrated gemini surfactant of known concentration (below and above the CMC 10–15 times) was added progressively. The maximum force with which the platinum ring was pulled out from the sample was noted to be the surface tension γ ($\text{mN}\cdot\text{m}^{-1}$) of the particular solution.

2.2.3. Fluorescence Measurements

All fluorescence spectra were measured using a Cary Eclipse Fluorescence (Agilent Technology) spectrophotometer. A strong hydrophobic fluorescent probe 1-pyrene carboxaldehyde (PyCHO) of 0.12 mM concentration was used in an aqueous micellar solution. The excitation wavelength was 334 nm and all fluorescence emission spectra were measured in the range of 340–450 nm. The excitation and emission slit widths were kept at 2.5 nm. Cetylpyridinium chloride (CPC) (0.12 mM) was used as the quencher to calculate the aggregation number.

2.2.4. FTIR Spectroscopy

The FTIR spectra of gemini surfactants and mixed systems were measured on a Bruker-ECO-ATR (attenuated total reflection) Model-i55 FTIR Spectrophotometer. In the mixed systems, the solid films were prepared via the evaporation of a 1:1 ratio water–ethanol solution by stirring the mixture for several minutes and allowing it to dry overnight at room temperature. All the spectra were obtained over the spectral range of $4000\text{--}400 \text{ cm}^{-1}$ at 298 K.

2.2.5. ^1H NMR Measurements

^1H NMR measurements were recorded using a Bruker Avance III NMR spectrometer (400 MHz) in D_2O .

2.2.6. Dynamic Light Scattering Study

The hydrodynamic diameter, size distribution and zeta potential of the aggregates were obtained using a Zetasizer Nano light scattering instrument (Malvern Instruments) with a He-Ne laser (633 nm, 10 mW). The scattering intensity was measured at $\theta = 173^\circ$. The data obtained were processed using the Malvern DTS Software 7.11 package.

3. Results and Discussion

3.1. Determination of the Critical Micelle Concentration

The CMC values were determined for both the gemini surfactants 16-10-16 and 16-12-16 in the presence of 0.2, 0.5, 0.7 and 1 wt% of 4-PyC8 using the conductivity and surface tension.

3.1.1. Conductivity

We investigated the aggregation properties of gemini surfactants in water in the presence and absence of the IL 4-PyC8. The breakpoint of the plot between the specific conductivity (κ) and gemini surfactant concentration gave the CMC of the gemini surfactant and mixed systems, see Figure 1. The aggregation of the surfactant formed at the breakpoint. The counter ion dissociation (α) of gemini surfactants for the pure and mixed system (gemini surfactants/IL 4-PyC8) were also evaluated (Table 1) from the ratio of the post-micellar and pre-micellar concentration range slopes obtained from the plots of specific conductance of the surfactant solution at different concentrations [41]:

$$\alpha = \frac{S_2}{S_1} \quad (1)$$

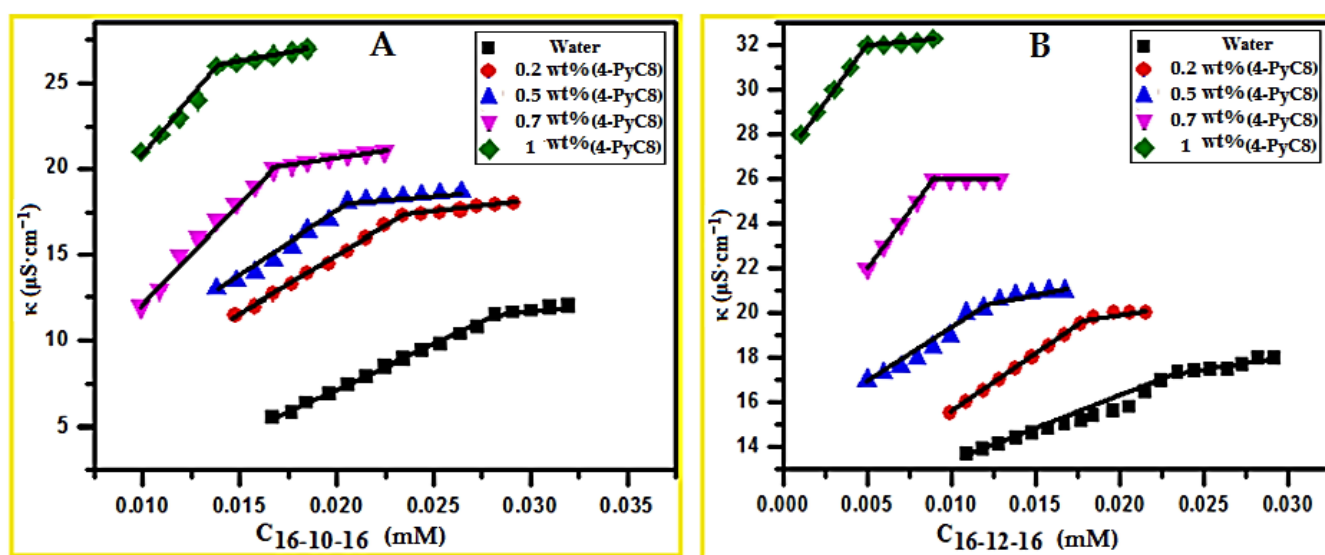


Figure 1. Specific conductivity ($\mu\text{S}\cdot\text{cm}^{-1}$) vs. concentration (mM) of the gemini surfactants 16-10-16 (A) and 16-12-16 (B) in the presence of 0.2, 0.5, 0.7 and 1 wt% of the IL 4-PyC8 at 300 K.

It was observed that on increasing the mass fraction of the IL 4-PyC8, the α values gradually decreased. The CMC and α values are listed in Table 1. It was observed that an increase in the concentration of the IL 4-PyC8 led to a sharp decrease in the CMC value for both gemini surfactants. Increasing the mass fraction of the IL 4-PyC8 lowered the electrostatic repulsion between the charged head groups of the gemini surfactant and reduced the CMC, which favored micellization [42,43].

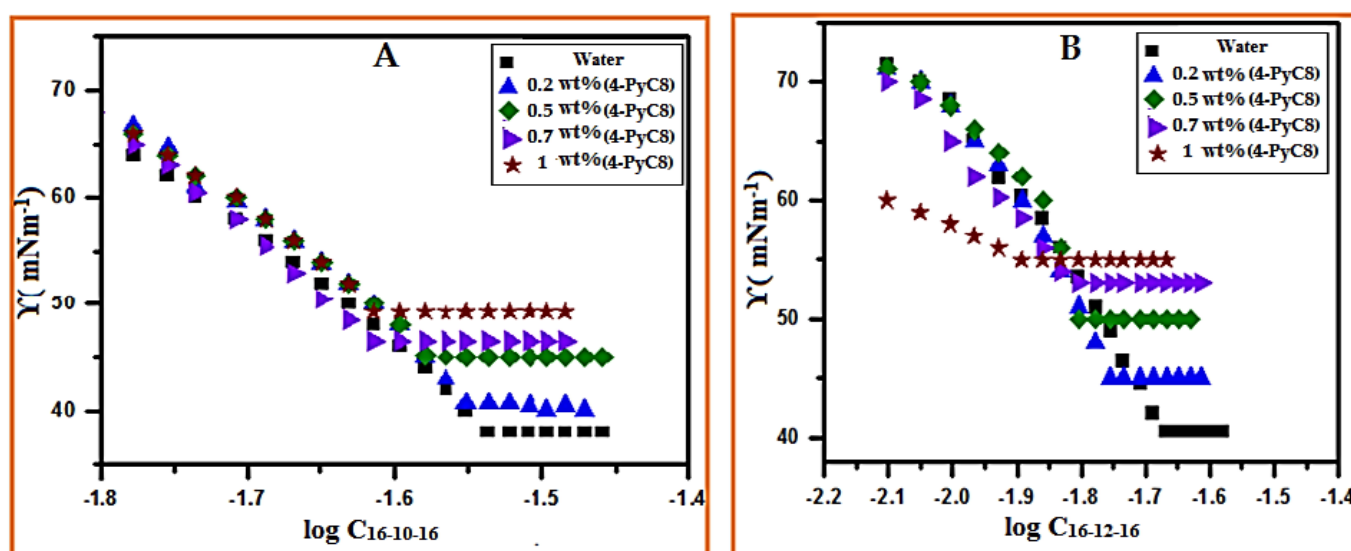
Table 1. Critical micelle concentration (CMC) and counter ion dissociation (α) of the gemini surfactants 16-s-16 with different contents (wt%) of the IL 4-PyC8 at 300 K.

IL 4-PyC8 (wt%)	CMC (mM)		
	Conductivity	Surface Tension	α
16-10-16			
Water	0.028 ^a	0.029	0.60
0.2	0.023	0.024	0.51
0.5	0.023	0.021	0.31
0.7	0.016	0.016	0.23
1.0	0.013	0.013	0.23
16-12-16			
Water	0.021 ^a	0.022	0.67
0.2	0.017	0.016	0.44
0.5	0.011	0.011	0.39
0.7	0.009	0.009	0.29
1.0	0.005	0.006	0.25

^a Ref [44].

3.1.2. Surface Tension

The surface tension versus the logarithm of the gemini surfactants concentration (M) plots are shown in Figure 2. The decrease in surface tension due to the adsorption of the gemini surfactant in the air/water interface is shown in Figure 2. At a constant gemini surfactant concentration, the surface tension gradually decreased when increasing the IL 4-PyC8 content. The surface tension decreased more rapidly, which may have been due to the longer alkyl chain IL increasing the hydrophobicity in the system [44,45]. Adding the IL 4-PyC8 caused the compression of the diffuse electric double layer, which decreased the electrostatic repulsions between the head groups of the gemini surfactants and reduced the CMC [46]. The CMC values obtained for the two gemini surfactants and mixed systems are listed in Table 1.

**Figure 2.** Surface tension vs. logarithm of the concentration of the gemini surfactants 16-10-16 (A) and 16-12-16 (B) in the presence of various mass fractions (0.2, 0.5, 0.7 and 1 wt%) of the IL 4-PyC8 at 300 K.

3.2. Effect of Oxime-Functionalized Ionic Liquid on the Interfacial Properties

The maximum surface excess (Γ_{\max}), minimum surface area per molecule (A_{\min}), surface tension at CMC (γ_{cmc}) and surface pressure at the CMC ($\Pi_{\text{cmc}} = \gamma_0 - \gamma_{\text{cmc}}$) of the

gemini surfactants in the presence of 4-PyC8 were determined using tensiometry. All these data are summarized in Table 2. The values of the maximum surface excess (Γ_{\max}) [33,47] were calculated using the Gibbs adsorption isotherm (Equation (2)):

$$\Gamma_{\max} = -\frac{1}{2.303nRT} \left[\frac{d\gamma}{d \log C} \right]_{T,P} \quad (2)$$

where $\frac{d\gamma}{d \log C}$ denotes the surface activity at a temperature (in Kelvin) and R is the universal gas constant ($8.314 \text{ J}\cdot\text{K}^{-1}\cdot\text{mol}^{-1}$). T is the absolute temperature in Kelvin, C is the concentration of the gemini surfactant and γ is the surface tension at a given concentration of surfactant. Since the gemini surfactant is made up of a divalent surfactant ion and two univalent counter-ions, the constant 'n' (pre-factor) value is taken as 3. The values of Γ_{\max} decreased with increasing the mass fraction of 4-PyC8 (Table 2). The values of the minimum area per molecule (A_{\min}) [33,48] of the gemini surfactant at the air-liquid interface were obtained using Equation (3):

$$A_{\min} = \frac{1}{\Gamma_{\max} \cdot N_A} \quad (3)$$

where N_A is the Avogadro's number ($6.022 \times 10^{23} \text{ mol}^{-1}$) and Γ_{\max} is the maximum surface excess concentration (mol m^{-2}) of adsorbed surfactant molecules at the interface. The A_{\min} values of the mixed systems composed of one of the two gemini surfactants and the IL 4-PyC8 are presented in Table 2. The results indicated that the values of Γ_{\max} and A_{\min} varied with the addition of the ionic liquid, revealing a lower Γ_{\max} (larger A_{\min}) with a higher content of IL. The values of Γ_{\max} decreased and A_{\min} increased due to the reduction in forces between the two head groups of the gemini surfactants in the presence of the IL 4-PyC8 when the molecules were less compactly packed at the air/water interface.

Table 2. Surface excess parameter (Γ_{\max}), surface pressure at CMC (π_{CMC}) and minimum surface area per molecule (A_{\min}) of the studied gemini surfactants for different mass fractions of the IL 4-PyC8 at 300 K.

IL 4-PyC8 (wt%)	γ_{CMC} ($\text{mN}\cdot\text{m}^{-1}$)	Γ_{\max} ($10^6 \text{ mol}\cdot\text{m}^{-2}$)	$10^{20} A_{\min}$ ($\text{m}^2 \text{ mol}^{-1}$)	π_{CMC} ($\text{mN}\cdot\text{m}^{-1}$)
16-10-16				
Water	38	2.10	79.18	34.1
0.2	41	1.30	128.36	31.4
0.5	45	1.22	135.75	27.1
0.7	46	1.19	139.04	25.6
1.0	49	0.99	167.09	22.9
16-12-16				
Water	40	1.99	83.88	31.0
0.2	45	1.27	131.45	26.5
0.5	50	1.26	132.04	21.5
0.7	53	1.20	138.21	18.5
1.0	55	0.93	178.72	16.5

Mean errors: $\gamma_{\text{cmc}} = \pm 1 \text{ mN}\cdot\text{m}^{-1}$, $\Gamma_{\max} = \pm 0.02 \text{ mol}\cdot\text{m}^{-2}$, $A_{\min} = \pm 0.02 \text{ m}^2 \text{ mol}^{-1}$, $\pi_{\text{CMC}} = \pm 0.10 \text{ mN}\cdot\text{m}^{-1}$.

The surface pressure at the CMC (π_{cmc}) [49] is a measure of the surface tension reduction at the CMC and is calculated using Equation (4):

$$\pi_{\text{CMC}} = \gamma_0 - \gamma_{\text{CMC}} \quad (4)$$

where γ_0 and γ_{cmc} correspond to pure water and the mixed system at the CMC at 300 K. The π_{cmc} values depend on the interfacial area occupied by the gemini surfactants with their specific position and the structure at the interface. The reduction of the surface tension

of the pure solvent by the gemini surfactants indicated more effective adsorption at the interface in the presence of the IL 4-PyC8 [33].

3.3. Effect of Oxime-Functionalized Ionic Liquid on Thermodynamic Parameters

Oxime-functionalized IL 4-PyC8 modified the physicochemical and thermodynamic properties of both gemini surfactants. The intermolecular forces, such as Van der Waals forces, dipole–dipole interaction and hydrogen bonding, were involved in the interaction of the IL 4-PyC8 with the gemini surfactants. The standard Gibbs free energy of micellization (ΔG°_m) was calculated for the analysis of the IL 4-PyC8 on the micellization process [50] using the following Equation (5):

$$\Delta G^\circ_m = 2(1.5 - \alpha) RT \ln X_{CMC} \quad (5)$$

where α is the degree of counterion dissociation, R is the ideal gas constant, T is the temperature in Kelvin and X_{CMC} is the CMC in the mole fraction unit.

The value of ΔG°_m became more negative as the IL 4-PyC8 concentration increased, which was due to stronger hydrophobic interactions. The calculated value of ΔG°_m is listed in Table 3. The negative value of ΔG°_m led to the spontaneous process. The standard Gibbs free energy of adsorption (ΔG°_{ads}) at the air/water interface [51] was calculated by using Equation (6):

$$\Delta G^\circ_{ads} = \frac{\Delta G^\circ_m - \pi_{CMC}}{\Gamma_{max}} \quad (6)$$

where ΔG°_m is the Gibbs free energy of micellization, Γ_{max} is the maximum surface excess concentration and π_{CMC} is the surface pressure at the CMC. Here, the addition of the IL 4-PyC8 led to an increase in ΔG°_{ads} , which indicated the stronger hydrophobic interaction due to the repulsion forces in the water/hydrophobic interface. The ΔG°_{ads} supported the micellization behavior between the IL 4-PyC8 and the gemini surfactants. The ΔG°_{ads} values also favored the spontaneous micellization process. All these values are listed in Table 3.

Table 3. Gibbs free energy of micellization (ΔG°_m), Gibbs free energy of micellization per alkyl tail ($\Delta G^\circ_{m,tail}$), Gibbs energy of transfer (ΔG°_{trans}), standard free energy of adsorption (ΔG°_{ads}) and Gibbs free energy of the given air/water interface ($\Delta G^{(s)}_{min}$) of the gemini surfactants 16-s-16 with different contents (wt%) of the IL 4-PyC8 at 300 K.

IL 4-PyC8 (wt%)	$\Delta G^{(s)}_{min}$ (kJ/mol)	ΔG°_m (kJ/mol)	$\Delta G^\circ_{m,tail}$ (kJ/mol)	ΔG°_{ads} (kJ/mol)	ΔG°_{trans} (kJ/mol)
16-10-16					
Water	18.12	−14.69	−7.34	−30.95	−
0.2	31.48	−16.55	−8.27	−40.82	−1.86
0.5	36.79	−20.23	−10.11	−42.40	−5.54
0.7	38.93	−22.10	−11.05	−43.55	−7.41
1.0	49.51	−22.68	−11.34	−45.74	−7.99
16-12-16					
Water	20.46	−14.11	−7.57	−29.69	−
0.2	35.62	−18.49	−9.24	−39.4	−4.38
0.5	39.76	−20.39	−10.10	−37.49	−6.28
0.7	44.12	−22.75	−11.30	−38.15	−8.64
1.0	59.19	−25.08	−12.50	−42.83	−10.97

Mean errors: $\Delta G^{(s)}_{min} = \pm 0.04$, $\Delta G^\circ_m = \pm 0.05$, $\Delta G^\circ_{m,tail} = \pm 0.04$, $\Delta G^\circ_{ads} = \pm 0.04$, $\Delta G^\circ_{trans} = \pm 0.04$.

The free energy of the given air/water interface $\Delta G^{(s)}_{min}$ [52] was found using Equation (7):

$$\Delta G^{(s)}_{min} = A_{min} \cdot \gamma_{CMC} \cdot N_A \quad (7)$$

$\Delta G_{\min}^{(s)}$ indicates the free energy change of the solution components from the bulk phase to the surface phase of the solution. Lower $\Delta G_{\min}^{(s)}$ values were reported to indicate [34] a more thermodynamically stable micellar surface. All thermodynamic parameters are given in Table 3. The Gibbs free energy of the micellization per alkyl tail may be expressed as (see Equation (8)) [53]:

$$\Delta G_{m,\text{tail}}^{\circ} = \frac{\Delta G_m^{\circ}}{2} \quad (8)$$

The gemini surfactant tail transfers Gibbs free energy from the solvent mixture to the hydrophobic core of the micelle. The tail of the gemini surfactant detached due to the solvophobic effects. The effect of the IL 4-PyC8 on the micellization process was also evaluated through the Gibbs energy of transfer ($\Delta G_{\text{trans}}^{\circ}$), given by Equation (9) [52]:

$$\Delta G_{\text{trans}}^{\circ} = \Delta G_m^{\circ}(\text{solvent mixed media}) - \Delta G_m^{\circ}(\text{pure water}) \quad (9)$$

As compared with the pure solvent, the addition of the IL 4-PyC8 made the thermodynamics more favorable for the gemini surfactant molecule and the hydrophobic tail part to move from the bulky phase into the micellar phase. As a result, $\Delta G_{\text{trans}}^{\circ}$ decreased with the decrease in the CMC values of the gemini surfactants.

3.4. Fluorescence Measurements

We used 1-pyrene carboxyaldehyde (PyCHO) as a fluorescence probe to obtain the CMC of the gemini surfactants in the presence and absence of the IL 4-PyC8. The fluorescence emission spectra exhibited a characteristic band near 450 nm. PyCHO fluorescence has been used to measure various important micellar parameters [54–56]. Fluorescence spectra were obtained from solutions of varying gemini surfactants in the presence of different mass fractions of the IL 4-PyC8. The CMC was determined by plotting the intensity against the gemini surfactant concentration (Figure 3). It is noteworthy to mention that the CMC of the gemini surfactants decreased with the increasing mass fraction of the IL 4-PyC8 (see Table 1). The CMC values determined using this method were slightly larger than those determined via the conductance and surface tension (see Table 1), which may have been due to the presence of the PyCHO in the micro-organized system [45,46].

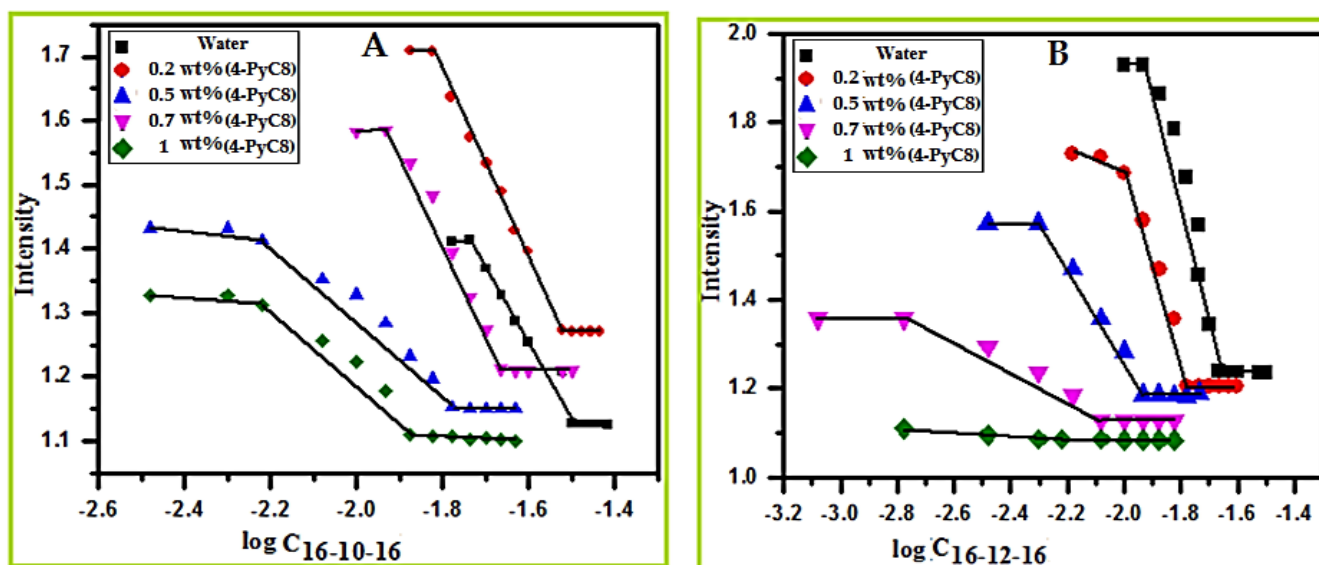


Figure 3. Intensity of the fluorescence vs. the logarithm of the concentration of the gemini surfactants 16-10-16 (A) and 16-12-16 (B) in water and in the presence of the IL 4-PyC8 at 300 K. The excitation wavelength was 334 nm and both excitation and emission slit widths were kept at 2 nm.

3.5. Aggregation Numbers

The aggregation behavior of the gemini surfactants and their interaction with the IL 4-PyC8 have also been studied via static fluorescence quenching measurements, which is a fundamental parameter of micellar properties, by using the following Equation (10):

$$\ln \left[\frac{I_0}{I_Q} \right] = \left[\frac{N_{\text{agg}}[Q]}{[\text{Surfactant}]_T - \text{CMC}} \right] \quad (10)$$

where $[Q]$ is the concentration of quencher (CPC), I_0 is the fluorescence intensities of pyrene with and without the quencher and $[\text{Surfactant}]_T$ is the total surfactant concentration. The plots of $\ln(I_0/I_Q)$ versus $[Q]$ for gemini surfactants 16-10-16 and 16-12-16 for different mass fractions of IL 4-PyC8 are shown in Figure 4. The aggregation numbers (N_{agg} 's) of the pure gemini surfactants and the mixed systems were determined from the slope of the plots of $\ln \left[\frac{I_0}{I_Q} \right]$ versus the quencher concentration. The aggregation number of the gemini surfactants decreased with increasing mass fraction of the IL 4-PyC8, which led to electrostatic repulsion and a hydrophobic effect between the head group of a surfactant and the charged ions (cations and anions) of the IL 4-PyC8 [57]. These factors held the micellization environment of the gemini surfactants in the presence of the IL 4-PyC8 [58]. We may suggest that between the two gemini surfactants, 16-12-16 was slightly more hydrophobic than 16-10-16, which resulted in the IL 4-PyC8 being able to transfer more successfully into the micelles of the gemini surfactant 16-10-16 [34].

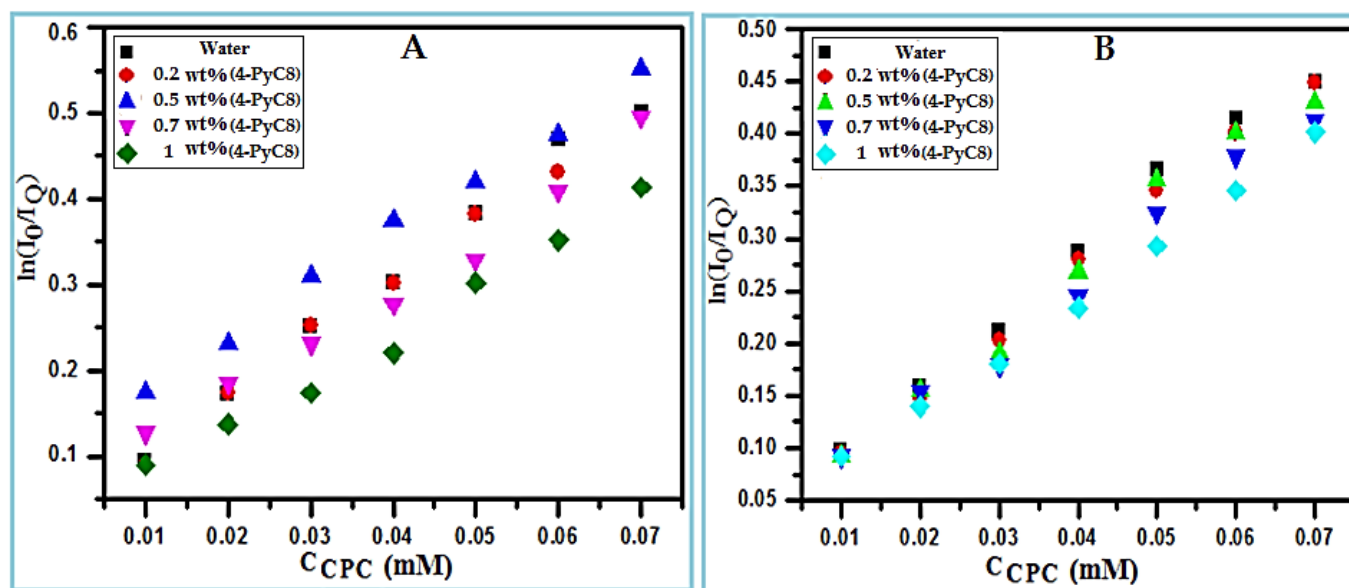


Figure 4. Plots of $\ln(I_0/I_Q)$ vs. concentration of CPC (0.12 mM) in different mass fractions of the IL 4-PyC8 at 300 K: (A) 16-10-16 and (B) 16-12-16. $[16-s-16] = 1$ mM.

The nature of the hydrophobicity of the gemini surfactants could be calculated using the Stern–Volmer quenching constant (K_{SV}) (Equation (11)). The K_{SV} values are given in Table 4.

$$\ln \left[\frac{I_0}{I_Q} \right] = 1 + K_{sv}[Q] \quad (11)$$

Table 4. Critical micelle concentration (CMC), aggregation number (N_{agg}) and Stern–Volmer constants (K_{SV}) of the two gemini surfactants 16-10-16 and 16-12-16 in water and in the presence of 0.2, 0.5, 0.7 and 1.0 wt% of the IL 4-PyC8 at 300 K.

IL 4-PyC8 (wt%)	CMC ^a (mM)	N_{agg}	K_{SV}
16-10-16			
Water	0.030 ^b	57	6.99
0.2	0.025	53	6.50
0.5	0.021	51	6.17
0.7	0.017	49	5.88
1.0	0.013	45	5.45
16-12-16			
Water	0.023 ^b	51	6.25
0.2	0.016	50	6.12
0.5	0.011	48	5.85
0.7	0.009	46	5.55
1.0	0.006	43	5.18

^a Fluorometry method, ^b Refs. [59,60].

The Stern–Volmer quenching constant (K_{SV}) can be assessed using the plots of $\ln(I_0/I_Q)$ versus $[Q]$. A difference in the K_{SV} values was observed, which can be explained using the base hydrophobicity of the micellar environment [55]. The higher the solubility of the probe and a quencher, the higher the K_{SV} value. The aggregation numbers and K_{SV} values are collected in Table 4.

The CMC values obtained using fluorometric techniques and collected in Table 4 were consistent with those obtained from the tensiometry and conductivity data (see Table 1).

3.6. FTIR Spectroscopy

The interaction between the oxime-functionalized IL 4-PyC8 and the gemini surfactants was studied using FTIR spectroscopy. The FTIR spectra of pure 16-s-16 and the IL 4-PyC8 are shown in Figures 5 and 6. In both spectra of 16-10-16 and 16-12-16, as well as for the IL 4-PyC8, there was no sharp peak at $\sim 3450\text{--}3700\text{ cm}^{-1}$, which shows that no water was present in the sample. The FTIR spectrum of 16-10-16 (Figure 5) showed a strong peak at the wavenumber 1467.97 cm^{-1} , which was due to C–N stretching. The different stretching bands observed were the symmetric and asymmetric stretching of the CH_2 vibration of alkyl chains at 2917.27 cm^{-1} and 2850.08 cm^{-1} , the symmetric and asymmetric stretching of the C–H scissoring vibration of the $\text{CH}_3\text{-N}^+$ moiety at 1467.97 cm^{-1} , the C–N⁺ stretching bands' rocking mode of the methylene chain at 889.09 cm^{-1} and the rocking mode of the methylene chain at 721.45 cm^{-1} . After the addition of the IL 4-PyC8, the stretching frequencies were changed to 2917.72 cm^{-1} , 2849.32 cm^{-1} , 1466.07 cm^{-1} , 889.75 cm^{-1} and 720.80 cm^{-1} , respectively. More importantly, the C=O stretching frequency for the IL 4-PyC8 at 1666 cm^{-1} was shifted to 1676 cm^{-1} after mixing with the gemini surfactant 16-10-16.

In the FTIR spectrum of the 16-12-16 gemini surfactant (shown in Figure 6), different frequencies were observed, see Table 5: symmetric and asymmetric stretching of the CH_2 vibration of alkyl chains at 2917.32 cm^{-1} and 2848.35 cm^{-1} , symmetric and asymmetric stretching of the C–H scissoring vibration of the $\text{CH}_3\text{-N}^+$ moiety at 1468.53 cm^{-1} , the C–N⁺ stretching bands' rocking mode of the methylene chain at 889.07 cm^{-1} and the rocking mode of the methylene chain at 721.96 cm^{-1} . For the mixture of the IL 4-PyC8 and gemini surfactants during the process of micellization, the stretching frequency values were changed to 2921.55 cm^{-1} , 2852.26 cm^{-1} , 1464.31 cm^{-1} , 889.60 cm^{-1} and 720.98 cm^{-1} , respectively. The shift of the wavenumber in the mixture of the gemini surfactant 16-12-16 and the IL 4-PyC8 represented some changes that occurred within the system. These variations in these peaks may have been due to +N-(CH₃) or NH₂ stretching. The observed difference in the wavenumber indicated that the additive IL 4-PyC8 interacted with the

gemini surfactants and it may have been due to some of the structural changes that occurred within the IL 4-PyC8:gemini surfactant mixed system. It is noteworthy that the C=O stretching frequency for 4-PyC8 at 1666 cm^{-1} was shifted to 1681 cm^{-1} after mixing with the gemini surfactant 16-12-16, indicating an IL:gemini surfactant mixed system. The changes in the IR spectra could be considered as non-specific interactions (ion–ion dipole and induced dipole interactions) between the gemini surfactants and IL that took part in the complexation, similar to what is reported in the literature [56] and in accordance with the ^1H NMR data discussed above.

Table 5. Infrared transmittance band and different modes of vibration of the gemini surfactants, 4-PyC8, and their mixtures.

Assignment	Band Position (cm^{-1})			
	16-10-16	16-10-16 + IL 4-PyC8	16-12-16	16-12-16 + IL 4-PyC8
Symmetric and asymmetric stretching of the C-H stretching vibration of the alkyl chains	2917.27, 2850.08	2917.72, 2849.32	2917.32, 2848.35	2921.55, 2852.26
Symmetric and asymmetric stretching of the C-H scissoring vibration of the $\text{CH}_3\text{-N}^+$ moiety	1467.97	1466.07	1468.53	1464.31
C-N ⁺ stretching bands' rocking mode of the methylene chain	889.09	889.75	889.07	889.60
Rocking mode of the methylene chain	721.45	720.80	721.96	720.98

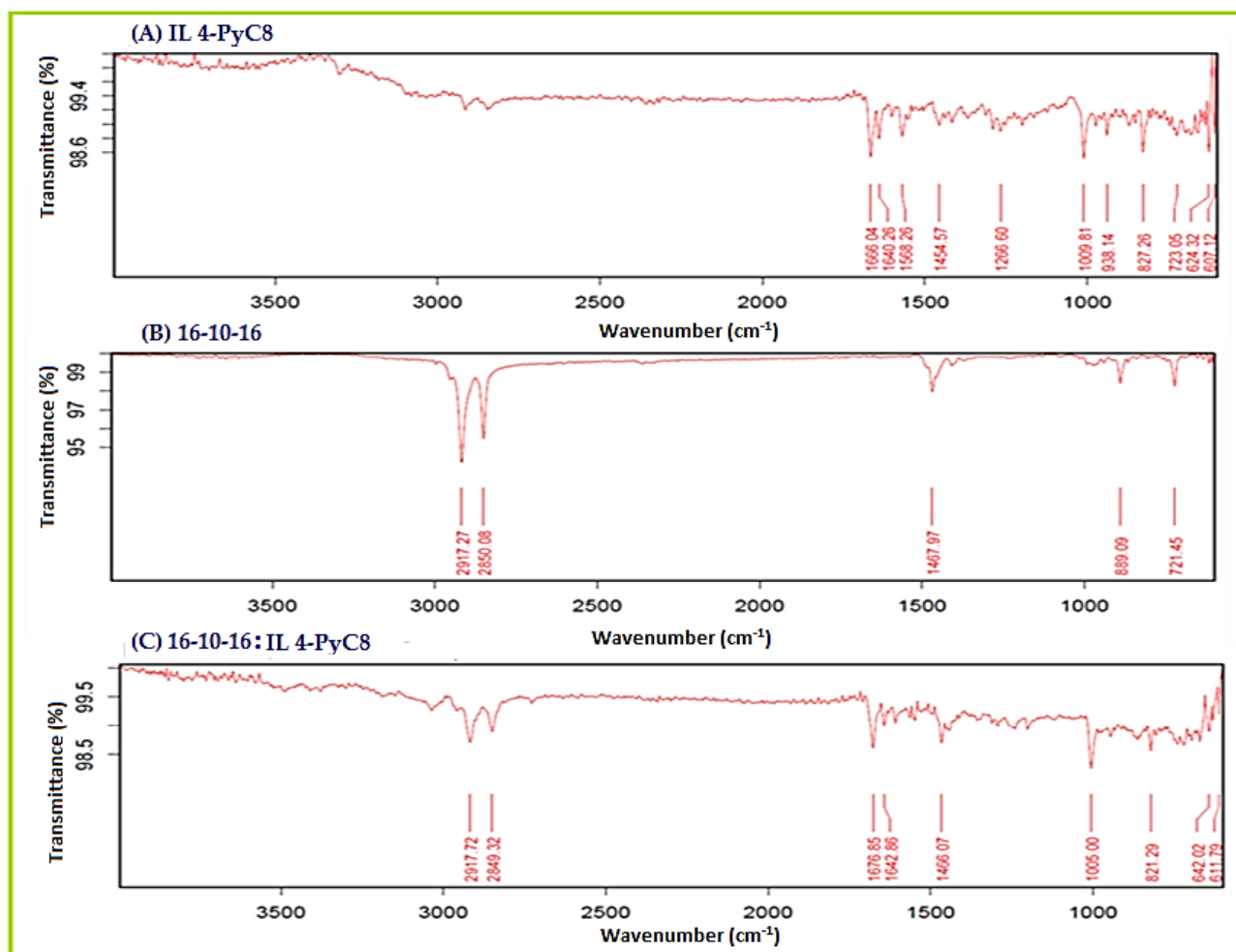


Figure 5. FTIR spectra of the (A) IL 4-PyC8, (B) 16-10-16 and (C) 16-10-16:IL 4-PyC8.

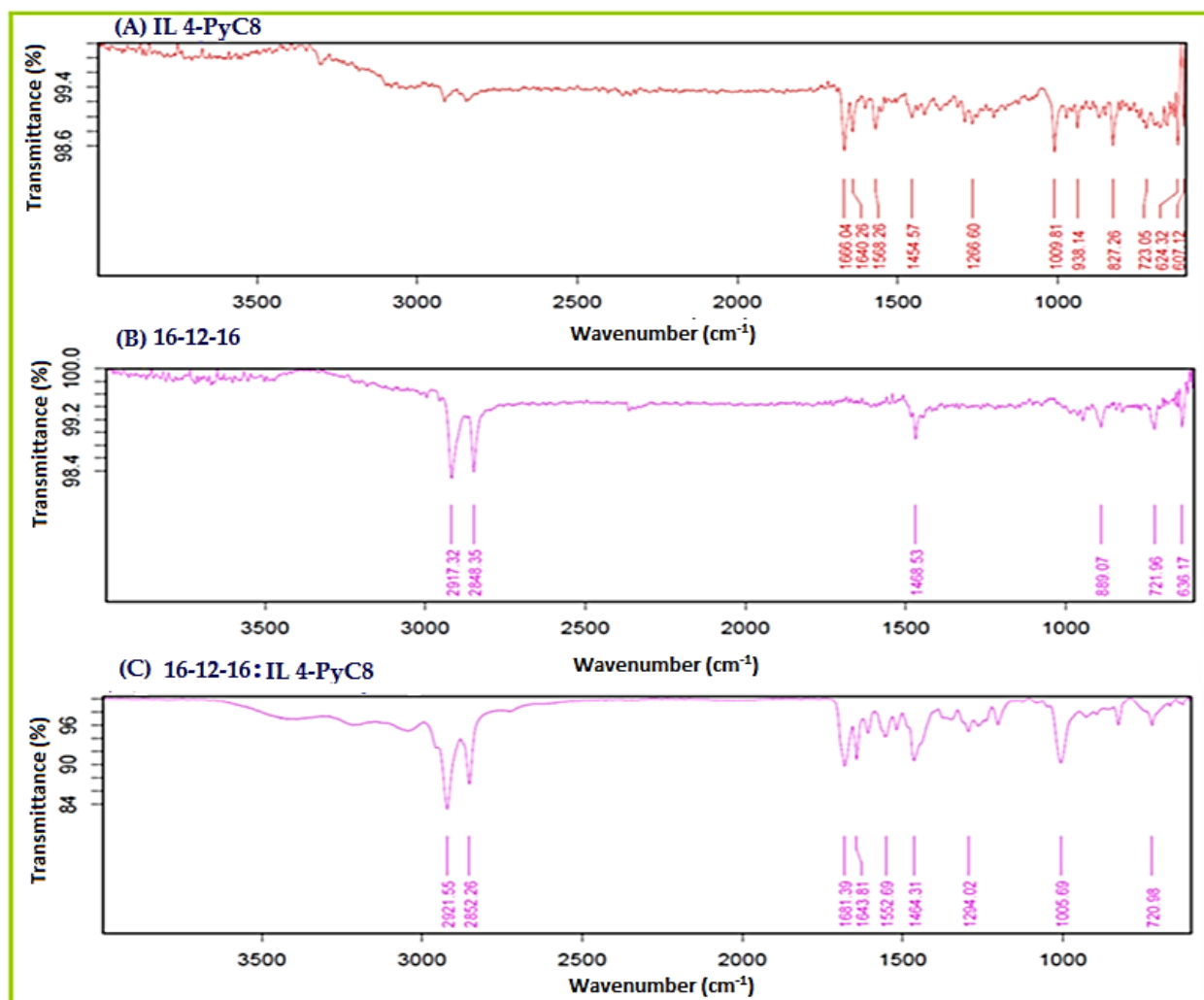


Figure 6. FTIR spectra of the (A) IL 4-PyC8, (B) 16-12-16 and (C) 16-12-16:IL 4-PyC8.

3.7. ¹H NMR Study

¹H NMR techniques are well-known to give information about the aggregate microenvironment and this can be used to probe the surfactant self-assembly of different structures [61]. Although NMR spectroscopy is a very useful technique, it can hardly be expected to recognize the changes in the chemical shifts of the side-chain protons. The hydrophobic tails form the micellar “core”, whereas the detectable changes in the chemical shifts occur mainly in the region close to the interface water/aggregate (e.g., micelle, vesicle). Aromatic protons can be very sensitive to the changes in the microenvironment of the surfactant aggregate [62]. Deprotonation of the oxime moiety due to changes in the micellar micropolarity or tight ion pair formation may also be detected using the changes in chemical shifts of the adjacent groups [61]. The ¹H NMR spectra of the gemini surfactants with the IL 4-PyC8 in D₂O are presented in Figure 7 (for 16-10-16) and Figure 8 (for 16-12-16). We note that no specific interaction confirmed by the changes in the chemical shifts could be reported based on these data; the surfactant aggregates were supposed to form under these concentration conditions, as gemini surfactants aggregates ([D]₀ >> CMC) with IL molecules were solubilized by the micelles.

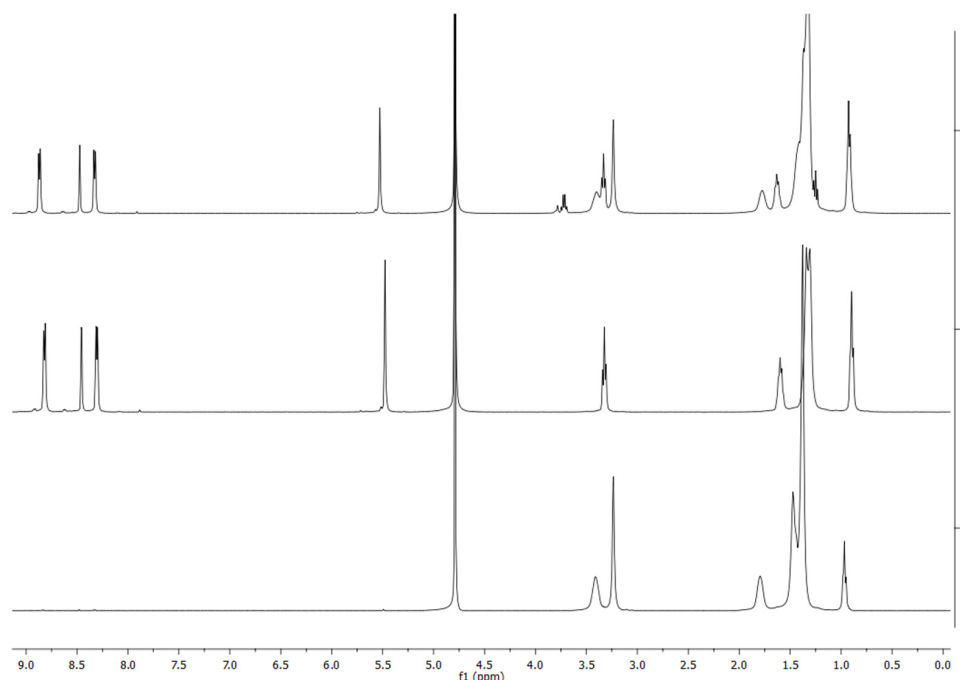


Figure 7. ^1H NMR spectra of the (1) 16-10-16, (2) IL 4-PyC8 and (3) 16-10-16:4-PyC8 in D_2O .

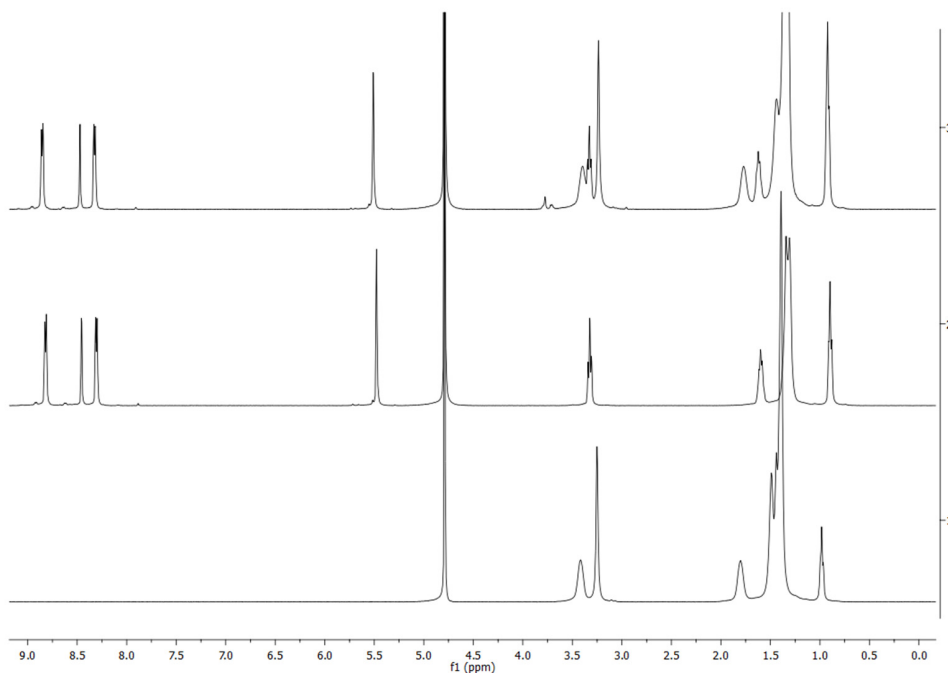


Figure 8. ^1H NMR spectra of the (1) 16-12-16, (2) IL 4-PyC8 and (3) 16-12-16:4-PyC8 in D_2O .

4. Dynamic Light Scattering and Zeta Potential Study of Mixed Gemini:IL System with PMZ

Taking into account the interactions between the oxime-derived IL and another phenothiazine drug called promazine that was reported recently [42], an evaluation of the structural changes of the aggregates of oxime IL/gemini surfactants with the addition of promethazine was carried out. Dynamic light scattering (DLS) studies were performed to shed light on the sizes of the self-assembly aggregates of the various concentrations of the IL 4-PyC8 that were added to the gemini surfactant solution in the presence of the drug PMZ. The aggregate size may be dependent on the solubilizate structure, as well as the nature and concentration of the surfactant, and using a low gemini concentration close to the CMC is not suitable since aggregates of different sizes and hardly defined

structures may form [63]. The concentration of the gemini surfactant 16-10-16 was taken significantly above the CMC value (1 mM). The DLS results provided us with information on the size of the gemini surfactant aggregates in the presence and absence of the drug and the IL 4-PyC8. It was observed that the hydrodynamic diameter of 1 mM aqueous gemini surfactant (ca. $35 \times$ CMC in the case of 16-10-16) solution without any other additives was observed to be about 124 nm (see Figure 9a), which was much larger than that of a regular spherical or ellipsoidal micelle [64]. Indeed, gemini surfactants are known to undergo a fast sphere-to-rod transition above the CMC [65], form unexpectedly large aggregates in the presence of polyaromatics [63,66,67] and to assemble into wormlike micelles [67], as well as other complex aggregates [68], at concentrations substantially above the CMC. As it was shown by Pisarcik et al. [69], the extension of the spacer length in the diamide gemini surfactant molecule to $s > 6$ results in a sharp increase in the N_{agg} with a concentration above the value of $2 \times$ CMC. Furthermore, surfactants with the spacer length of $n = 8$ were reported to form aggregates of >100 nm at the concentration of $6 \times$ CMC. Since the aggregation numbers were not large enough to expect vesicle formation, Pisarcik et al. [69] suggested the hydrodynamic size reflected the intermicellar aggregates. We supposed the 16-10-16 surfactants reported in the present work may demonstrate similar behavior at the studied concentration. An addition of PMZ (0.01 mM) to the gemini micellar solution resulted in a significant increase in the aggregate size from 124 nm to 270 nm. It is noteworthy to mention that the addition of 1 wt% of the oxime-functionalized IL 4-PyC8 to the above gemini micellar solutions with the drug added resulted in a drastic structural transition from such larger aggregates of 270 nm to small-sized micelles with sizes of 1 to 2 nm (see Figure 9f). The size distribution at 1–2 nm might correspond to the micelles but is smaller than the real size of the micelles in this technique, which may be ascribed to the high charge density of the gemini surfactant micelles that affects the DLS measurement [70]. Initially, the addition of the drug produced a significant increase in the micellar size due to the partition of the drug within the (inter)micellar aggregate interior region, but the addition of the IL 4-PyC8 to this system caused drastic changes in the micellar size of the gemini:IL:PMZ system. These changes in the self-assembly structural transition may indicate stronger IL:PMZ, gemini:IL and gemini:PMZ interactions.

The values of the zeta potential measurement (ξ (mV)) in these systems depend on the difference in potential between the dispersion medium and on the stationary liquid layer that is attached to the dispersed aggregates [71]. Initially, the value of ξ insignificantly increased with the addition of drug (24.8 mV) to the gemini micellar solution (22.6 mV), reflecting the positive charges on the overall surface of the carrier. Upon the addition of IL4-PyC8 to the gemini:PMZ system, the value of ξ slightly decreased (Table 6). This may have reflected the strong electrostatic interactions that took place between the oppositely charged ions present within the micellar system [72]. As a result, a different self-assembly shape appeared, which caused the lowering of the values of ξ [63,73]. Further, adding higher concentrations of the IL 4-PyC8 (1.0 wt%) into the mixture of the gemini:PMZ solution resulted in an increase in the surface charge density. The overall strong interactions (16-s-16:IL:PMZ) led to the significant structural changes of gemini aggregates in the presence of 1 wt% of the oxime-functionalized IL 4-PyC8 to the gemini surfactant solutions with the drug added. There was a correlation between the surface potential and the aggregates' sizes and morphologies, as the aggregates were formed with varying morphologies [74] in the presence of the drug and the IL 4-PyC8.

Table 6. Micellar size *d* (nm) as a size distribution by number and zeta potential in the presence of various concentrations of the IL 4-PyC8 in the drug PMZ and the gemini micellar solution.

System Composition	Aggregate Characteristics	
	<i>d</i> (nm)	Zeta Potential, ξ (mV)
16-10-16 (1 mM)	124 (105–164)	22.6
16-10-16 + PMZ (0.01 mM)	270 (220–395)	24.8
16-10-16 + PMZ + 0.1 wt% IL4-PyC8	210 (165–255), 825 (615–1105)	24.1
16-10-16 + PMZ + 0.5 wt% IL4-PyC8	182 (142–220)	20.6
16-10-16 + PMZ + 1.0 wt% IL4-PyC8	1.4 (1.1–1.8)	23.7

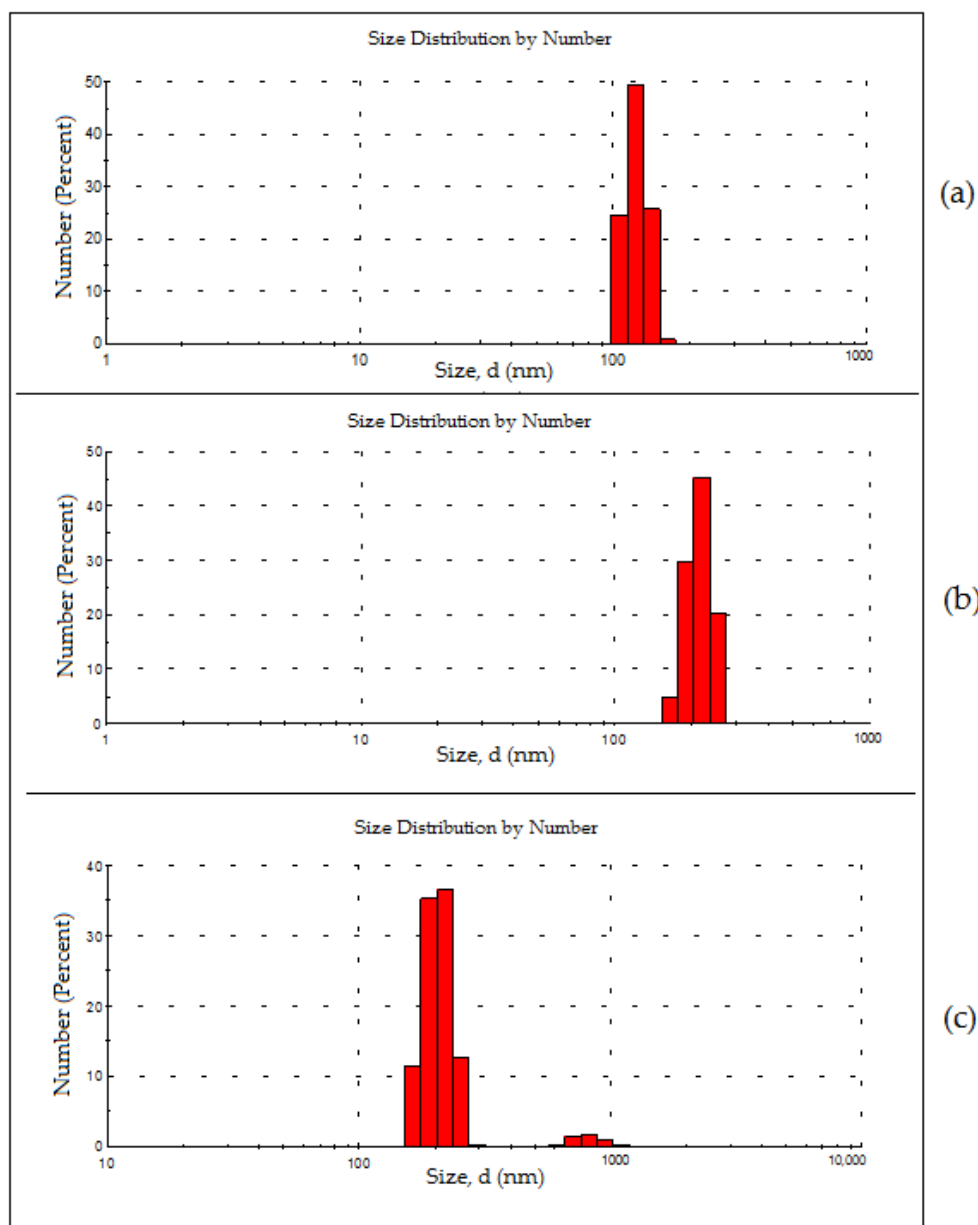


Figure 9. Cont.

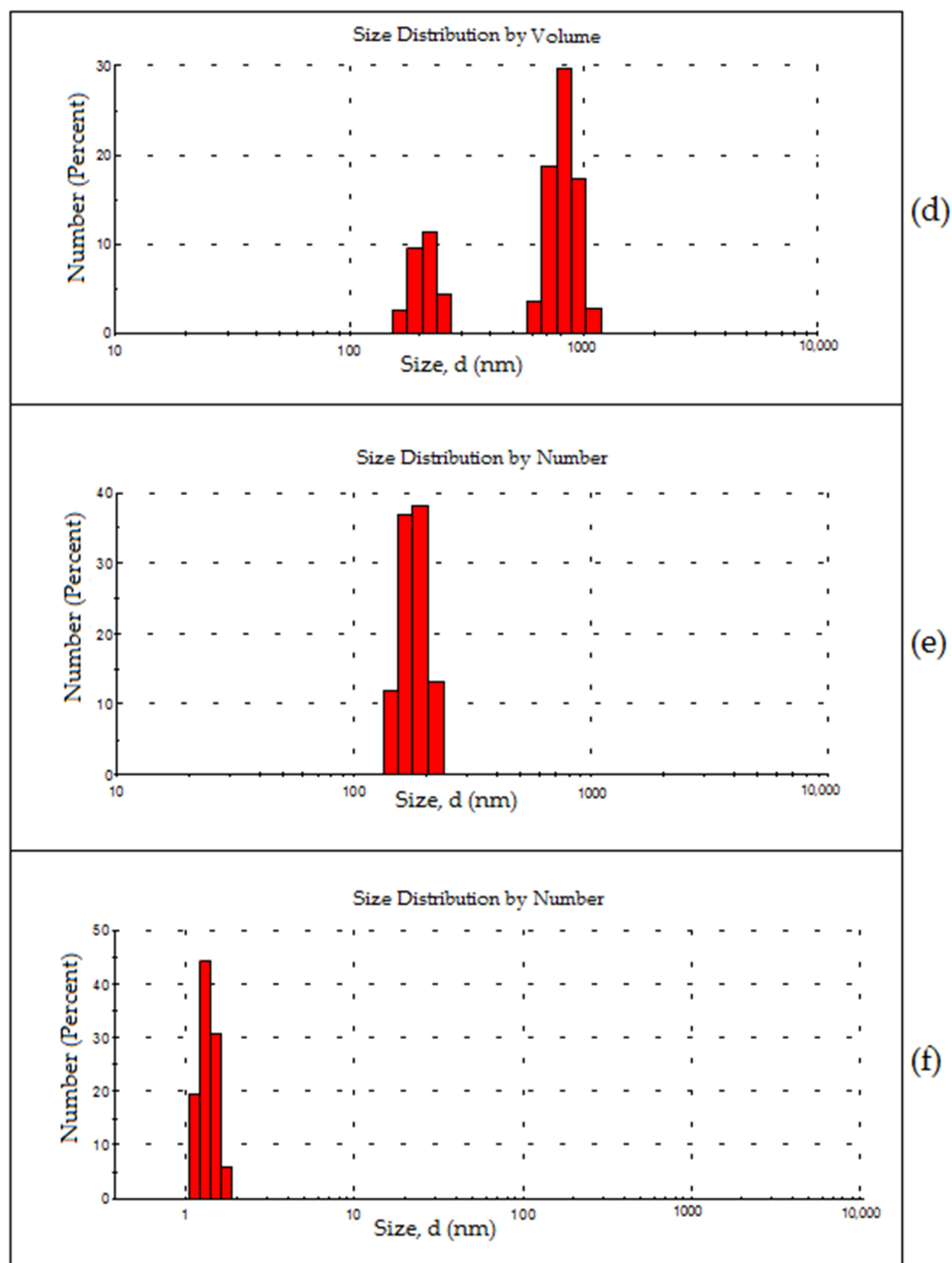


Figure 9. Aggregates size distribution obtained from DLS for various concentrations of the IL 4-PyC8 in drug PMZ and gemini surfactant 16-10-16: (a) 16-10-16 (without additives), (b) 16-10-16:PMZ, (c,d) 16-10-16:PMZ:0.1 wt% IL 4-PyC8, (e) 16-10-16:PMZ:0.5 wt% IL 4-PyC8 and (f) 16-10-16:PMZ:1.0 wt% IL 4-PyC8.

5. Conclusions

The design and application of sustainable surfactants in the remediation of contaminated areas were considered regarding promethazine, a chiral pharmaceutical pollutant. The micellization behavior and physicochemical properties of the gemini surfactants 16-10-16 and 16-12-16 in the presence of the functionalized IL 4-PyC8 were investigated using surface tension, conductivity, fluorescence, FTIR, ^1H NMR and DLS techniques. The surface tension and conductometry results revealed a decrease in the CMC of both the gemini surfactants in the presence of the IL 4-PyC8, thus favoring the micelle formation process. The negative values of ΔG_m^0 and ΔG_{ads}^0 indicated that the micellization process

was spontaneous. The aggregation number (N_{agg}) and Stern–Volmer constant (K_{SV}) of the gemini surfactants decreased with the increasing mass fraction of the IL 4-PyC8. The cmc and N_{agg} results may be ascribed to the presence of counterions near the polar heads of the gemini surfactant molecules that tended to decrease the electrostatic repulsion forces between the gemini surfactant head groups, leading to the compact aggregation of surfactant monomers. The aggregate sizes obtained from the DLS measurements demonstrated that the addition of 1 wt% of the oxime-functionalized IL 4-PyC8 to the gemini surfactant solutions in the presence of promethazine may have resulted in a structural transition from very large aggregates (270 nm) to small compact micelles following strong gemini:IL:PMZ interactions. The structural transitions in the presence of promethazine reported in the present work may be used for designing systems responsive to changes in the size and shape of the aggregates as an analytical signal for the selective binding of biologically important molecules and potential chiral pollutants.

Author Contributions: Conceptualization and idea of the research, Y.K.; K.K.G. and V.B.; synthesis of compounds, methodology, I.V.K.; experimental techniques, data curation analysis of the results, conceptualization, methodology, S.J.P., M.K.B. and K.B.; analysis and interpretation, M.K.B., I.V.K.; formal analysis and interpretation, K.B.; writing—original draft preparation, S.J.P.; writing—review and editing, I.V.K., Y.K., V.B.; funding acquisition, Y.K., K.K.G. and V.B. All authors have read and agreed to the published version of the manuscript.

Funding: This work was supported by a DST-FIST grant (no. SR/FST/CSI-259/2014(C)) and UGC-SAP-DRS-II (for K.K.G. and S.J.P.), European Union’s H2020-FETOPEN grant 828779 (INITIO) (for V.B.), NATO SPS MYP no. G5565 (DEFIR) (for Y.K.), Estonian Research Council grants ETAG20049 (COVSG5) (for Y.K.) and PRG399 (for V.B.).

Institutional Review Board Statement: Not applicable.

Informed Consent Statement: Not applicable.

Data Availability Statement: All the data gathered for this study are available in the article.

Acknowledgments: The authors are grateful to the National Center for Natural Resources (NCNR), Pt. Ravishankar Shukla University, Raipur (C.G.), for providing the FTIR and NMR facilities.

Conflicts of Interest: The authors declare no conflict of interest.

References

1. Hembury, G.A.; Borovkov, V.V.; Inoue, Y. Chirality sensing supramolecular systems. *Chem. Rev.* **2008**, *108*, 1–73. [[CrossRef](#)] [[PubMed](#)]
2. Konrad, N.; Horetski, M.; Sihtmae, M.; Truong, K.-N.; Osadchuk, I.; Burankova, T.; Kielmann, M.; Adamson, J.; Kahru, A.; Rissanen, K.; et al. Thiourea organocatalysts as emerging chiral pollutants: En route to porphyrin-based (chir)optical sensing. *Chemosensors* **2021**, *9*, 278. [[CrossRef](#)]
3. Shtykov, S. (Ed.) *Nanoanalytics: Nanoobjects and Nanotechnologies in Analytical Chemistry*; Walter de Gruyter GmbH: Berlin, Germany, 2018; p. 463.
4. Patel, M.; Kumar, R.; Kishor, K.; Mlsna, T.; Pittman, C.U., Jr.; Mohan, D. Pharmaceuticals of Emerging Concern in Aquatic Systems: Chemistry, Occurrence, Effects, and Removal Methods. *Chem. Rev.* **2019**, *119*, 3510–3673. [[CrossRef](#)] [[PubMed](#)]
5. Zakharova, L.Y.; Serdyuk, A.A.; Mirgorodskaya, A.B.; Kapitanov, I.V.; Gainanova, G.A.; Karpichev, Y.; Gavrilova, E.L.; Sinyashin, O.G. Amino acid-functionalized calix [4]resorcinarene solubilization by mono-and dicationic surfactants. *J. Surfactants Deterg.* **2016**, *19*, 493–499. [[CrossRef](#)]
6. Rasheed, T.; Shafi, S.; Bilal, M.; Hussain, T.; Sherd, F.; Rizwan, K. Surfactants-based remediation as an effective approach for removal of environmental pollutants—A review. *J. Mol. Liq.* **2020**, *318*, 113960. [[CrossRef](#)]
7. Anastas, P.; Eghbali, N. Green Chemistry: Principles and Practice. *Chem. Soc. Rev.* **2010**, *39*, 301–312. [[CrossRef](#)]
8. Ranke, J.; Stolte, S.; Stormann, R.; Arning, J.; Jastorff, B. Design of sustainable chemical products—The example of ionic liquids. *Chem. Rev.* **2007**, *107*, 2183–2206. [[CrossRef](#)]
9. Clarke, C.J.; Tu, W.-C.; Levers, O.; Bröhl, A.; Hallett, J.P. Green and Sustainable Solvents in Chemical Processes. *Chem. Rev.* **2018**, *118*, 747–800. [[CrossRef](#)]
10. Sheldon, R.A. Green solvents for sustainable organic synthesis: State of the art. *Green Chem.* **2005**, *7*, 267–278. [[CrossRef](#)]
11. MacFarlane, D.R.; Chong, A.L.; Forsyth, M.; Kar, M.; Vijayaraghavan, R.; Somers, A.; Pringle, J.M. New dimensions in salt-solvent mixtures: A 4th evolution of ionic liquids. *Faraday Discuss.* **2018**, *206*, 9–28. [[CrossRef](#)]

12. Egorova, K.S.; Gordeev, E.G.; Ananikov, V.P. Biological Activity of Ionic Liquids and Their Application in Pharmaceuticals and Medicine. *Chem. Rev.* **2017**, *117*, 7132–7189. [[CrossRef](#)] [[PubMed](#)]
13. Aldous, L.; Khan, A.; Hossain, M.M.; Zhao, C.; C Hardacre, V.P. *Catalysis in Ionic Liquids: From Catalyst Synthesis to Application*; Royal Society of Chemistry: London, UK, 2014; Volume 15, pp. 1–620.
14. Bica, K.; Gartner, P.; Gritsch, P.J.; Ressmann, A.K.; Schroder, C.; Zirbs, R. Micellar catalysis in aqueous-ionic liquid systems. *Chem. Commun.* **2012**, *48*, 5013–5015. [[CrossRef](#)] [[PubMed](#)]
15. Steinruck, H.P.; Wasserscheid, P. Ionic Liquids in Catalysis. *Catal. Lett.* **2015**, *145*, 380–397. [[CrossRef](#)]
16. Han, X.; Armstrong, D.W. Ionic liquids in separations. *Acc. Chem. Res.* **2007**, *40*, 1079–1086. [[CrossRef](#)] [[PubMed](#)]
17. Smiglak, M.; Metlen, A.; Rogers, R.D. The second evolution of ionic liquids: From solvents and separations to advanced materials-energetic examples from the ionic liquid cookbook. *Acc. Chem. Res.* **2007**, *40*, 1182–1192. [[CrossRef](#)]
18. Torimoto, T.; Tsuda, T.; Okazaki, K.; Kuwabata, S. New Frontiers in Materials Science Opened by Ionic Liquids. *Adv. Mater.* **2010**, *22*, 1196–1221. [[CrossRef](#)]
19. Jordan, A.; Haib, A.; Spulak, M.; Karpichev, Y.; Kummerer, K.; Gathergood, N. Synthesis of a Series of Amino Acid Derived Ionic Liquids and Tertiary Amines: Green chemistry metrics including microbial toxicity and preliminary biodegradation data analysis. *Green Chem.* **2016**, *18*, 4374–4392. [[CrossRef](#)]
20. Garcia, M.T.; Ribosa, I.; Perez, L.; Manresa, A.; Comelles, F. Aggregation Behavior and Antimicrobial Activity of Ester-Functionalized Imidazolium- and Pyridinium-Based Ionic Liquids in Aqueous Solution. *Langmuir* **2013**, *29*, 2536–2545. [[CrossRef](#)]
21. Teresa Garcia, M.; Ribosa, I.; Perez, L.; Manresa, A.; Comelles, F. Self-assembly and antimicrobial activity of long-chain amide-functionalized ionic liquids in aqueous solution. *Colloids Surf. B Biointerfaces* **2014**, *123*, 318–325. [[CrossRef](#)]
22. Haiss, A.; Jordan, A.; Westphal, J.; Logunova, E.; Gathergood, N.; Kummerer, K. On the way to greener ionic liquids: Identification of a fully mineralizable phenylalanine-based ionic liquid. *Green Chem.* **2016**, *18*, 4361–4373. [[CrossRef](#)]
23. Kusumahastuti, D.K.A.; Sihtmae, M.; Kapitanov, I.V.; Karpichev, Y.; Gathergood, N.; Kahru, A. Toxicity profiling of 24 L-phenylalanine derived ionic liquids based on pyridinium, imidazolium and cholinium cations and varying alkyl chains using rapid screening *Vibrio fischeri* bioassay. *Ecotoxicol. Environ. Saf.* **2019**, *172*, 556–565. [[CrossRef](#)] [[PubMed](#)]
24. Kapitanov, I.; Jordan, A.; Karpichev, Y.; Spulak, M.; Perez, L.; Kellett, A.; Kummerer, K.; Gathergood, N. Synthesis, self-assembly, antimicrobial activity, and preliminary biodegradation studies of a series of L-phenylalanine-derived surface active ionic liquids. *Green Chem.* **2019**, *21*, 1777–1794. [[CrossRef](#)]
25. Suk, M.; Haiss, A.; Westphal, J.; Jordan, A.; Kellett, A.; Kapitanov, I.; Karpichev, Y.; Gathergood, N.; Kummerer, K. Design rules for environmental biodegradability of phenylalanine alkyl ester linked ionic liquids for green chemistry. *Green Chem.* **2020**, *22*, 4498–4508. [[CrossRef](#)]
26. Pandya, S.J.; Kapitanov, I.V.; Usmani, Z.; Sahu, R.; Sinha, D.; Gathergood, N.; Ghosh, K.K.; Karpichev, Y. An example of green surfactant systems based on inherently biodegradable IL-derived amphiphilic oximes. *J. Mol. Liq.* **2020**, *305*, 112857. [[CrossRef](#)]
27. Pal, B.K.; Moulik, S.P. *Ionic Liquid-Based Surfactant Science: Formulation, Characterization, and Applications*; John Wiley & Sons Inc.: Hoboken, NJ, USA, 2015; p. 576.
28. Chen, L.G.; Strassburg, S.H.; Bermudez, H. Micelle co-assembly in surfactant/ionic liquid mixtures. *J. Colloid Interface Sci.* **2016**, *477*, 40–45. [[CrossRef](#)]
29. Kumar, A.; Banjare, M.K.; Sinha, S.; Yadav, T.; Sahu, R.; Satnami, M.L.; Ghosh, K.K. Imidazolium-Based Ionic Liquid as Modulator of Physicochemical Properties of Cationic, Anionic, Nonionic, and Gemini Surfactants. *J. Surfactants Deterg.* **2018**, *21*, 355–366. [[CrossRef](#)]
30. Shang, Y.Z.; Wang, T.F.; Han, X.; Peng, C.J.; Liu, H.L. Effect of Ionic Liquids C(n)mimBr on Properties of Gemini Surfactant 12-3-12 Aqueous Solution. *Ind. Eng. Chem. Res.* **2010**, *49*, 8852–8857. [[CrossRef](#)]
31. El Seoud, O.; Keppeler, N.; Malek, N.I.; Galdano, P.D. Ionic Liquid-Based Surfactants: Recent Advances in Their Syntheses, Solution Properties, and Applications. *Polymers* **2021**, *13*, 1100. [[CrossRef](#)]
32. Menger, F.M.; Keiper, J.S. Gemini surfactants. *Angew. Chem. Int. Ed.* **2000**, *39*, 1907–1920. [[CrossRef](#)]
33. Zana, R. Dimeric and oligomeric surfactants. Behavior at interfaces and in aqueous solution: A review. *Adv. Colloid Interface Sci.* **2002**, *97*, 205–253. [[CrossRef](#)]
34. Zana, R. Gemini (dimeric) surfactants. *Curr. Opin. Colloid Interface Sci.* **1996**, *1*, 566–571. [[CrossRef](#)]
35. Akram, M.; Anwar, S. Biophysical investigation of promethazine hydrochloride binding with micelles of biocompatible gemini surfactants: Combination of spectroscopic and electrochemical analysis. *Spectrochim. Acta Part A Mol. Biomol. Spectrosc.* **2019**, *215*, 249–259. [[CrossRef](#)] [[PubMed](#)]
36. Ferraz, R.; Branco, L.C.; Prudencio, C.; Noronha, J.P.; Petrovski, Z. Ionic Liquids as Active Pharmaceutical Ingredients. *ChemMedChem* **2011**, *6*, 975–985. [[CrossRef](#)] [[PubMed](#)]
37. Ozan, M.; Gokturk, S. Effect of ionic liquids as active pharmaceutical ingredients on the micellar binding of an amphiphilic drug trifluopromazine hydrochloride. *J. Dispers. Sci. Technol.* **2019**, *14*, 214–222. [[CrossRef](#)]
38. Mahajan, S.; Sharma, R.; Mahajan, R.K. An investigation of drug binding ability of a surface active ionic liquid: Micellization, electrochemical, and spectroscopic studies. *Langmuir* **2012**, *28*, 17238–17246. [[CrossRef](#)]
39. Mahajan, S.; Sharma, R.; Mahajan, R.K. Interactions of new 1,8-diazabicyclo[5.4.0]undec-7-ene (DBU) based surface active ionic liquids with amitriptyline hydrochloride: Micellization and interfacial studies. *Colloids Surf. A Physicochem. Eng. Asp.* **2013**, *424*, 96–104. [[CrossRef](#)]

40. Banjare, M.K.; Behera, K.; Banjare, R.K.; Pandey, S.; Ghosh, K.K.; Karpichev, Y. Molecular interactions between novel synthesized biodegradable ionic liquids with antidepressant drug. *Chem. Thermodyn. Therm. Anal.* **2021**, *3*, 100012. [[CrossRef](#)]
41. Pal, M.; Rai, R.; Yadav, A.; Khanna, R.; Baker, G.A.; Pandey, S. Self-aggregation of sodium dodecyl sulfate within (choline chlo-ride+urea) deep eutectic solvent. *Langmuir* **2014**, *30*, 13191–13198. [[CrossRef](#)]
42. Sun, T.; Gao, S.; Chen, Q.; Shen, X. Investigation on the interactions between hydrophobic anions of ionic liquids and Triton X-114 micelles in aqueous solutions. *Colloids Surf. A Physicochem. Eng. Asp.* **2014**, *456*, 18–25. [[CrossRef](#)]
43. Abdul Rub, M. Aggregation and interfacial phenomenon of amphiphilic drug under the influence of pharmaceutical excipients (green/biocompatible gemini surfactant). *PLoS ONE* **2019**, *14*, e0211077. [[CrossRef](#)]
44. Khan, I.A.; Mohammad, R.; Alam, M.S.; Kabir-ud-Din. Effect of alkylamine chain length on the critical micelle concentration of cationic Gemini butanediyl-a,x-bis(dimethylcetylammmonium bromide) surfactant. *J. Dispers. Sci. Technol.* **2009**, *30*, 1486–1493. [[CrossRef](#)]
45. Markiewicz, R.; Klimaszuk, A.; Jarek, M.; Taube, M.; Florczak, P.; Kempka, M.; Fojud, Z.; Jurga, S. Influence of Alkyl Chain Length on Thermal Properties, Structure, and Self-Diffusion Coefficients of Alkyltriethylammmonium-Based Ionic Liquids. *Int. J. Mol. Sci.* **2021**, *22*, 5935. [[CrossRef](#)] [[PubMed](#)]
46. Khan, F.; Siddiqui, U.S.; Khan, I.A. Physicochemical study of cationic Gemini surfactant butanediyl-1,4- bis(dimethyldodecylammmonium bromide) with various counterions in aqueous solution. *Colloids Surf. A Physicochem. Eng. Asp.* **2012**, *394*, 46–56. [[CrossRef](#)]
47. Wattebled, L.; Laschewsky, A. Effects of organic salt additives on the behavior of dimeric (“Gemini”) surfactants in aqueous solution. *Langmuir* **2007**, *23*, 10044–10052. [[CrossRef](#)] [[PubMed](#)]
48. Huddleston, J.G.; Visser, A.E.; Reichert, W.M.; Willauer, H.D.; Broker, G.A.; Rogers, R.D. Characterization and comparison of hydrophilic and hydrophobic room temperature ionic liquids incorporating the imidazolium cation. *Green Chem.* **2001**, *3*, 156–164. [[CrossRef](#)]
49. Tikariha, D.; Singh, N.; Satnami, M.L.; Ghosh, K.K.; Barbero, N.; Quagliotto, P. Physicochemical characterization of cationic Gemini surfactants and their effect on reaction kinetics in ethylene glycol–water medium. *Colloids Surf. A Physicochem. Eng. Asp.* **2012**, *411*, 1–11. [[CrossRef](#)]
50. Comelles, F.; Ribosa, I.; Gonzalez, J.J.; Garcia, M.T. Micellization of sodium laurylthoxy sulfate (SLES) and short chain imidazolium ionic liquids in aqueous solution. *J. Colloid Interface Sci.* **2014**, *425*, 44–45. [[CrossRef](#)]
51. Wang, X.; Yan, F.; Li, Z.; Zhang, L.; Zhao, S.; An, J.; Jiayong, Y. Synthesis and surface properties of several nonionic–anionic surfactants with straight chain alkyl-benzyl hydrophobic group. *Colloids Surf. A Physicochem. Eng. Asp.* **2007**, *302*, 532–539. [[CrossRef](#)]
52. Li, N.; Gao, Y.A.; Zheng, L.; Zhang, J.; Yu, L.; Li, X. Studies on the micro polarities of bmimBF₄/TX-100/toluene ionic liquid microemulsions and their behaviors characterized by UV–visible spectroscopy. *Langmuir* **2007**, *23*, 1091–1097. [[CrossRef](#)]
53. Bhaire, M.L.; Pandey, S.; Khan, M.S.; Talib, A.; Wu, H.F. Fluorophotometric determination of critical micelle concentration (CMC) of ionic and non-ionic surfactants with carbon dots via Stokes shift. *Talanta* **2015**, *132*, 572–578. [[CrossRef](#)]
54. More, U.; Kumari, P.; Vaid, Z.; Behra, K.; Malek, N.I. Interaction between ionic liquids and Gemini surfactant: A detailed investigation into the role of ionic liquids in modifying properties of aqueous Gemini surfactant. *J. Surfactants Deterg.* **2016**, *19*, 75–89. [[CrossRef](#)]
55. Palchowdhury, S.; Bhargava, B.L. Effect of cation asymmetry on the aggregation in aqueous 1-alkyl, 3-decylimidazolium bromide solutions: Molecular dynamics studies. *J. Phys. Chem. B* **2014**, *118*, 6241–6249. [[CrossRef](#)] [[PubMed](#)]
56. Banjare, M.K.; Kurrey, R.; Yadav, T.; Sinha, S.; Satnami, M.L.; Ghosh, K.K. A comparative study on the effect of imidazolium-based ionic liquid on self-aggregation of cationic, anionic and nonionic surfactants studied by surface tension, conductivity, fluorescence and FTIR spectroscopy. *J. Mol. Liq.* **2017**, *241*, 622–632. [[CrossRef](#)]
57. Ba-Salem, A.O.; Duhamel, J. Determination of the Aggregation Number of Pyrene-Labeled Gemini Surfactant Micelles by Pyrene Fluorescence Quenching Measurements. *Langmuir* **2021**, *37*, 6069–6079. [[CrossRef](#)] [[PubMed](#)]
58. Gargi, B.R.; Indranil, C.; Satya, P.M. Pyrene absorption can be a convenient method for probing critical micellar concentration (CMC) and indexing micellar polarity. *J. Colloid Interface Sci.* **2006**, *294*, 248–254.
59. Karpovich, D.S.; Blanchard, G.J. Relating the polarity-dependent fluorescence response of pyrene to vibronic coupling. Achieving a fundamental understanding of the pyrene polarity scale. *J. Phys. Chem.* **1995**, *99*, 3951–3958. [[CrossRef](#)]
60. Dong, D.C.; Winnik, M.A. The py scale of solvent polarities. *Can. J. Chem.* **1984**, *62*, 2560–2565. [[CrossRef](#)]
61. Derman, O.S.; Stilbs, P.; Price, W.S. NMR Studies of Surfactants. *Concepts Magn. Reson. Part A Educ. J.* **2004**, *23*, 121–135. [[CrossRef](#)]
62. Savsunenko, O.; Matondo, H.; Messant, S.F.; Perez, E.; Popov, A.F.; Lattes, I.R.; Lattes, A.; Karpichev, Y. Functionalized vesicles based on amphiphilic boronic acids: A system for recognizing biologically important polyols. *Langmuir* **2013**, *29*, 3207–3213. [[CrossRef](#)]
63. Serdyuk, A.A.; Mirgorodskaya, A.B.; Kapitanov, I.V.; Gathergood, N.; Zakharova, L.Y.; Sinyashin, O.G.; Karpichev, Y. Effect of structure of polycyclic aromatic substrates on solubilization capacity and size of cationic monomeric and gemini 14-s-14 surfactant aggregates. *Colloids Surf. A Physicochem. Eng. Asp.* **2016**, *509*, 613–622. [[CrossRef](#)]
64. Desnoyers, J.E.; Perron, G. Temperature dependence of the free energy of micellization from calorimetric data. *Langmuir* **1996**, *12*, 4044–4045. [[CrossRef](#)]
65. Devinsky, F.; Masarova, L.; Lacko, I. Surface activity and micelle formation of some new bisquaternary ammonium salts. *J. Colloid Interface Sci.* **1985**, *105*, 235–239. [[CrossRef](#)]

66. Shafi, M.; Bhat, P.A.; Dar, A.A. Solubilization capabilities of mixtures of cationic Gemini surfactant with conventional cationic, nonionic and anionic surfactants towards polycyclic aromatic hydrocarbons. *J. Hazard. Mater.* **2009**, *167*, 575–581.
67. Li, Q.; Wang, X.; Yue, X.; Chen, X. Wormlike micelles formed using Gemini surfactants with quaternary hydroxyethyl methylammonium headgroups. *Soft Matter* **2013**, *9*, 9667–9674. [[CrossRef](#)]
68. Mahajan, S.; Mahajan, R.K. Interactions of phenothiazine drugs with bile salts: Micellization and binding studies. *J. Colloid Interface Sci.* **2012**, *387*, 194–204. [[CrossRef](#)]
69. Pisarcik, M.; Polakovicova, M.; Markuliak, M.; Lukac, M.; Devinsky, F. Self-Assembly Properties of Cationic Gemini Surfactants with Biodegradable Groups in the Spacer. *Molecules* **2019**, *24*, 1481. [[CrossRef](#)]
70. Yu, D.; Huang, X.; Deng, M.; Lin, Y.; Jiang, L.; Huang, J.; Wang, Y.; Zana, R. Effects of Inorganic and Organic Salts on Aggregation Behavior of Cationic Gemini Surfactants. *J. Phys. Chem. B* **2010**, *114*, 14955–14964. [[CrossRef](#)]
71. Oliver, R.C.; Lipfert, J.; Fox, D.A.; Lo, R.H.; Doniach, S.; Columbus, L. Dependence of Micelle Size and Shape on Detergent Alkyl Chain Length and Head Group. *PLoS ONE* **2013**, *8*, 62488–62497. [[CrossRef](#)]
72. Ghosh, S.; Roy, A.; Banik, D.; Kundu, N.; Kuchlyan, J.; Dhir, A.; Sarkar, N. How Does the Surface Charge of Ionic Surfactant and Cholesterol Forming Vesicles Control Rotational and Translational Motion of Rhodamine 6G Perchlorate (R6G ClO₄)? *Langmuir* **2015**, *31*, 2310–2320. [[CrossRef](#)]
73. Geng, Y.; Romsted, L.S.; Menger, F. Specific ion pairing and interfacial hydration as controlling factors in gemini micelle morphology. Chemical trapping studies. *J. Am. Chem. Soc.* **2006**, *128*, 492–501. [[CrossRef](#)]
74. Zana, R. Dimeric (gemini) surfactants: Effect of the spacer group on the association behavior in aqueous solution. *J. Colloid Interface Sci.* **2002**, *248*, 203–220. [[CrossRef](#)] [[PubMed](#)]